Supplementary Information (SI) for Journal of Materials Chemistry B.

Supporting Information

Low-cost, robust, and transportable devices based on Cu(I)-I cluster hybrid luminescent compound as tetracycline sensors for contaminated waters

Elena de la Rubia[a], *Ricardo Garsed*[a], *Fernando Aguilar-Galindo*[b,d], *Andrea Garcia-Hernán*[a], *Gines Lifante-Pedrola*[c], *Pilar Amo-Ochoa*[a,d]*.

[a] *Dpto. de Química Inorgánica. Universidad Autónoma de Madrid, 28049 Madrid, Spain.*

[b] *Dpto. Química. Universidad Autónoma de Madrid, 28049 Madrid, Spain*

[c] *Dpto. de Física de Materiales. Universidad Autónoma de Madrid, 28049 Madrid, Spain.*

[d] *Institute for Advanced Research in Chemical Sciences (IAdChem). Universidad Autónoma de Madrid, 28049 Madrid, Spain*

Characterization of the 1-propyl-1,4-diazabicyclo[2.2.2]octan-1-ium (pr-ted) ligand

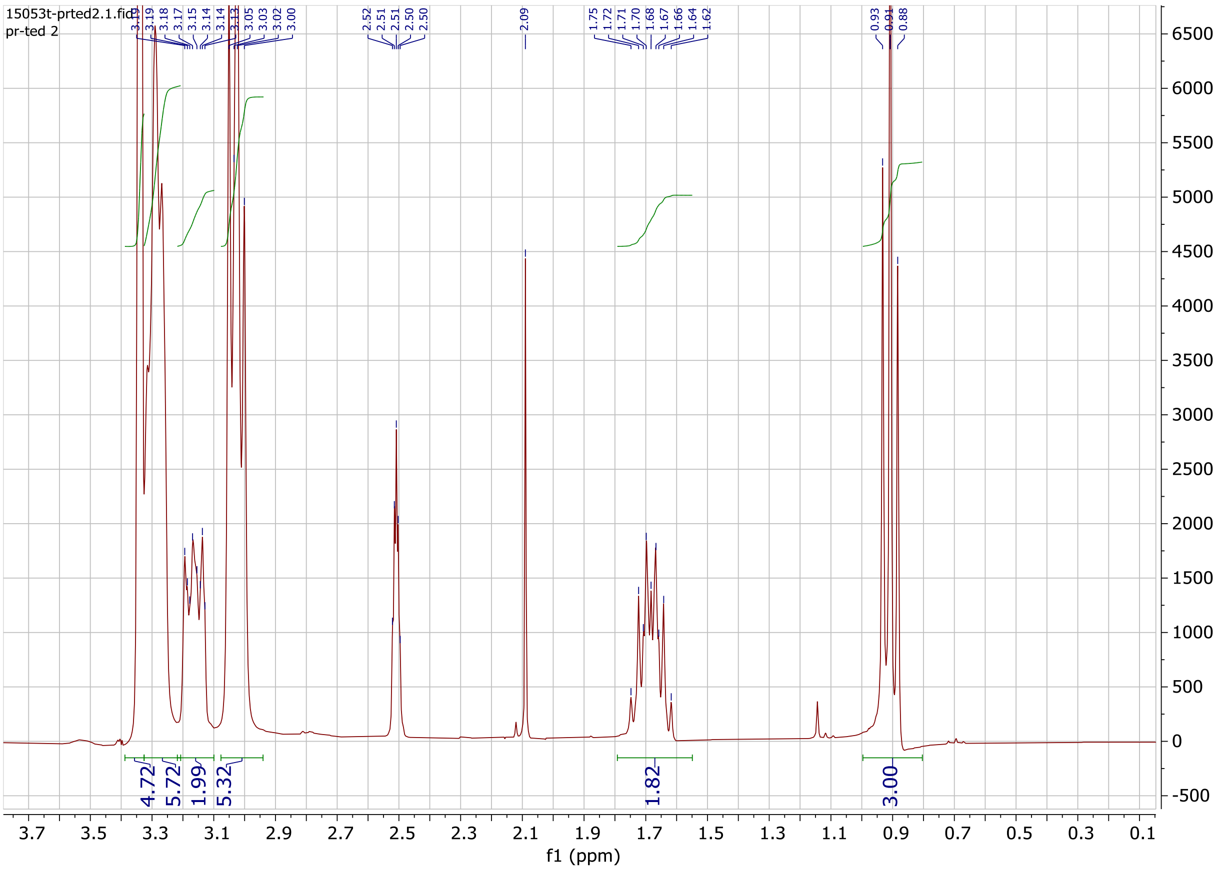

Figure S1: [1]H-NMR spectrum for 1-propyl-1,4-diazabicyclo[2.2.2]octan-1-ium (pr-ted) ligand in CD_3CN.

Characterization of submicrometric [Cu_4I_6(pr-ted)$_2$] particles

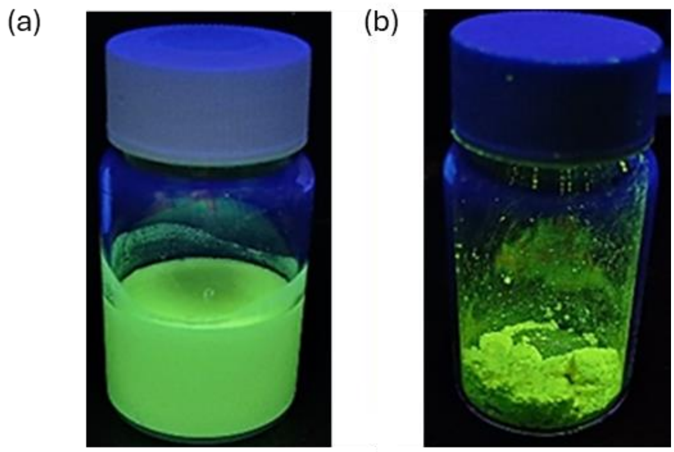

Figure S2: Images of [Cu_4I_6(pr-ted)$_2$] particles suspended in ethanol (a) and particles after filtration (b). Under ultraviolet light (λ= 365nm).

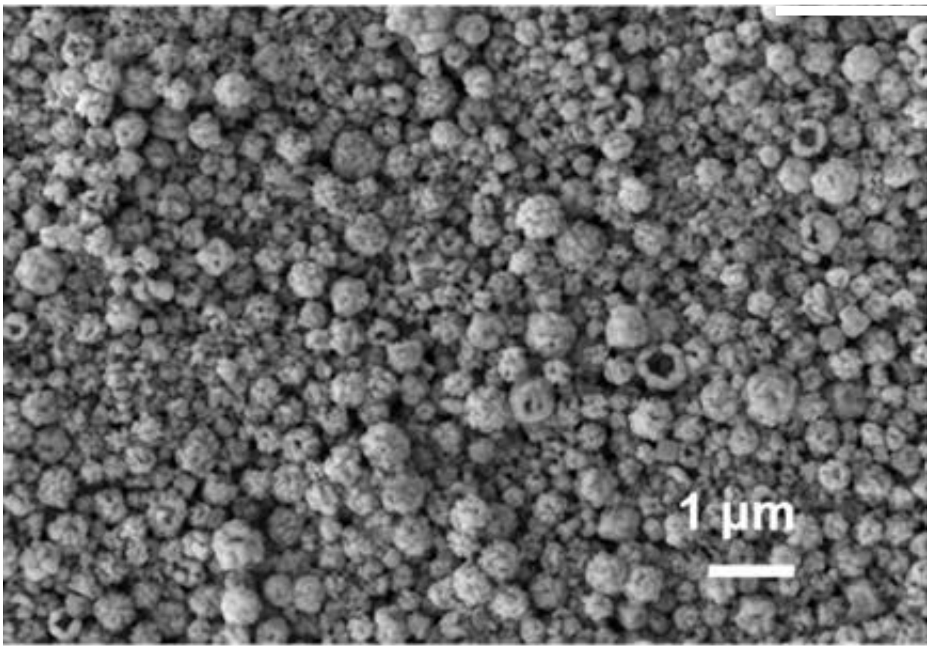

Figure S3: SEM image of submicrometric [Cu_4I_6(pr-ted)$_2$] particles. The average size of [Cu_4I_6(pr-ted)$_2$] particles is 369.2 ± 129.5 nm.

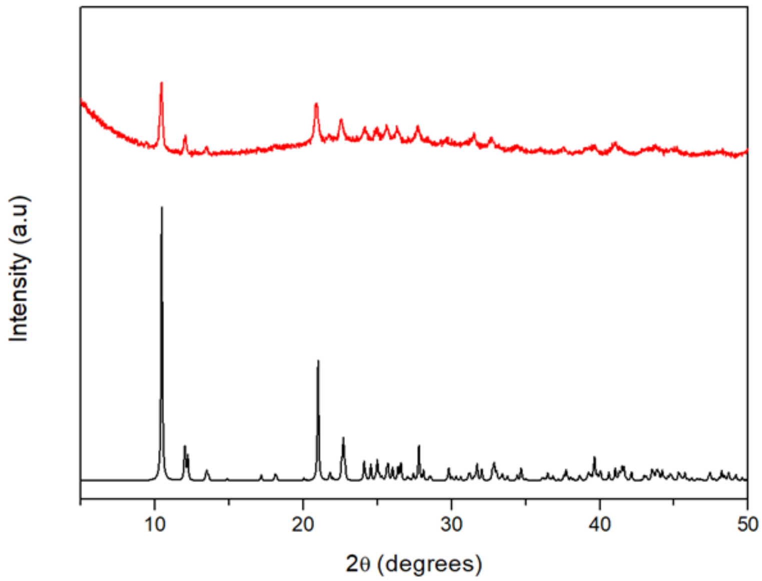

Figure S4: Simulated PXRD diffraction pattern of [Cu_4I_6(pr-ted)$_2$] from single crystal (black) and PXRD diffraction pattern of submicromertric [Cu_4I_6(pr-ted)$_2$] particles (red).

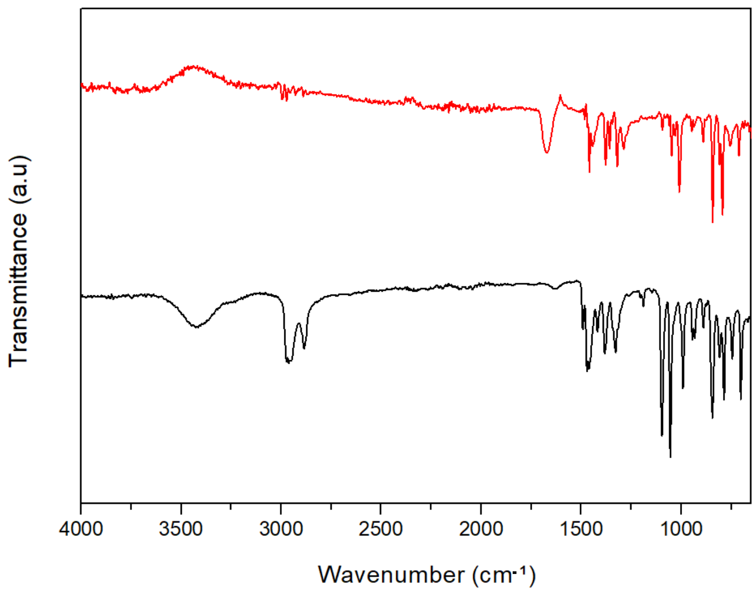

Figure S5: ATR-FTIR spectra of 1-propyl-1,4-diazabicyclo[2.2.2]octan-1-ium (pr-ted) (black) and submicrometric [Cu_4I_6(pr-ted)$_2$] particles (red).

Table S1. DLS size of submicrometric [Cu_4I_6(pr-ted)$_2$] particles in different solvents (ethanol and water).

Solvent	Water	Ethanol
Size (nm)	841.0	495,2

Water stability studies of submicrometric [Cu_4I_6(pr-ted)$_2$] particles as a function of time and pH.

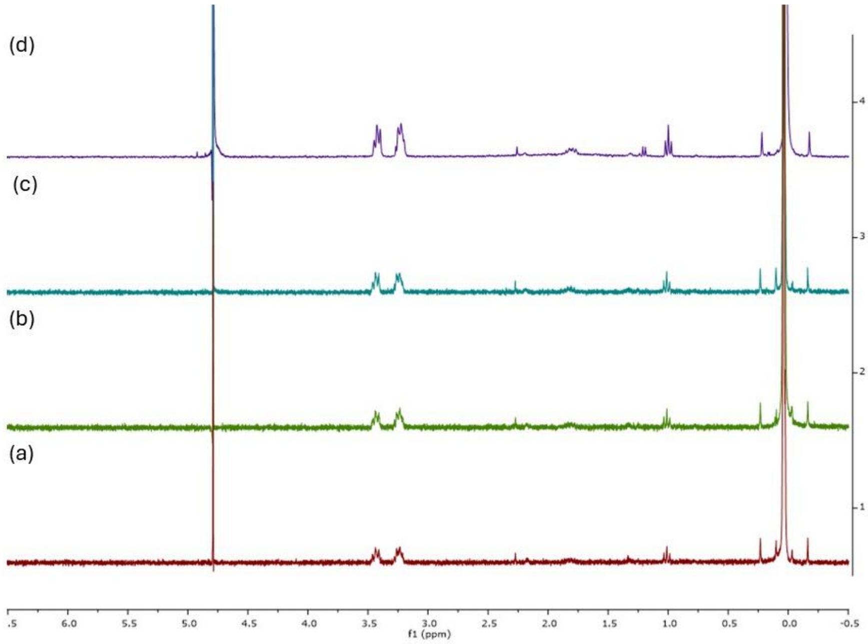

Figure S6. ^{1}H-NMR of submicrometric [Cu_4I_6(pr-ted)$_2$] particles in D_2O at initial time (a), after 1 hour (b), after 1 day (c), and after 7 days (d).

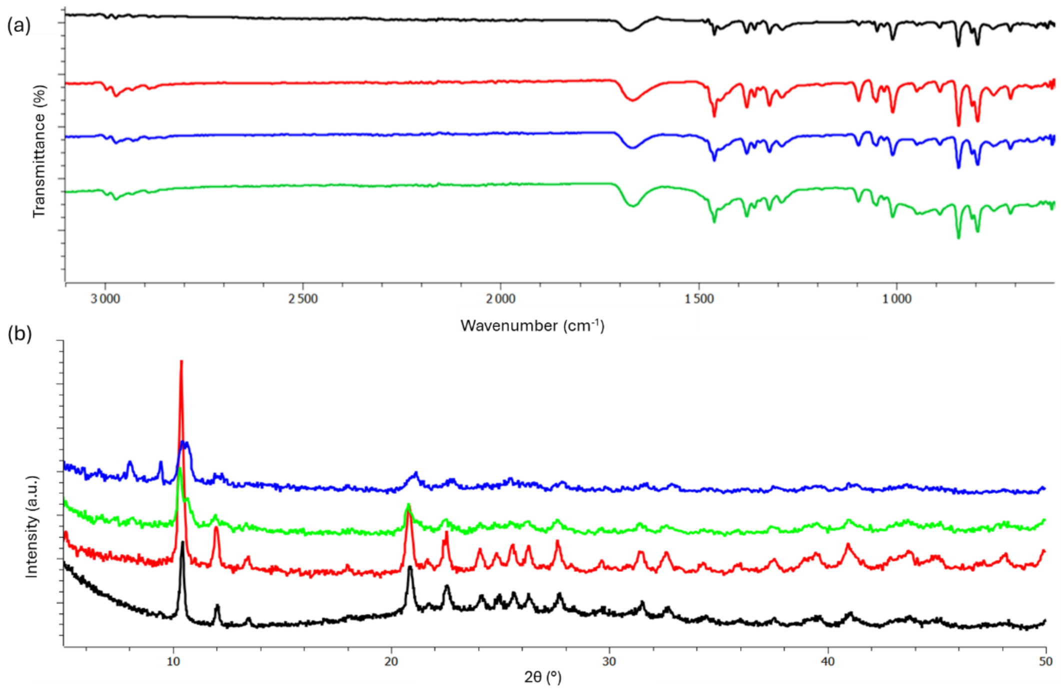

Figure S7: a) ATR-FTIR and b) PXRD spectrum of submicrometric [Cu_4I_6(pr-ted)$_2$] particles (black), at pH= 8.89 (red), pH= 7.30 (green) and pH= 4.24 (blue).

Sensing versus tetracycline (TC).

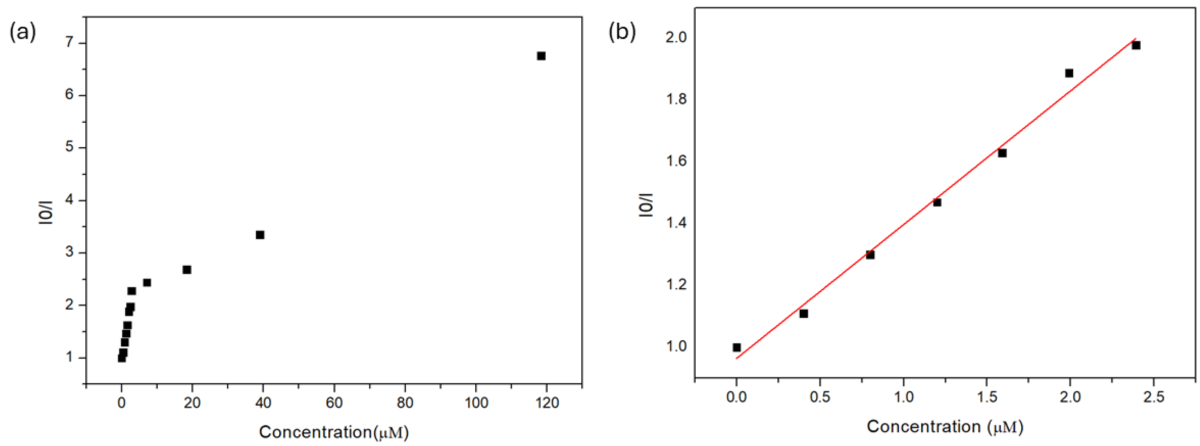

Figure S8: S-V plot for the quenching of the emission of the aqueous suspension of submicron $[Cu_4I_6(pr\text{-}ted)_2]$ particles in the presence of TC (a) and expanded Stern-Volmer plot in the linear range 0 - 2.5 μM (b).

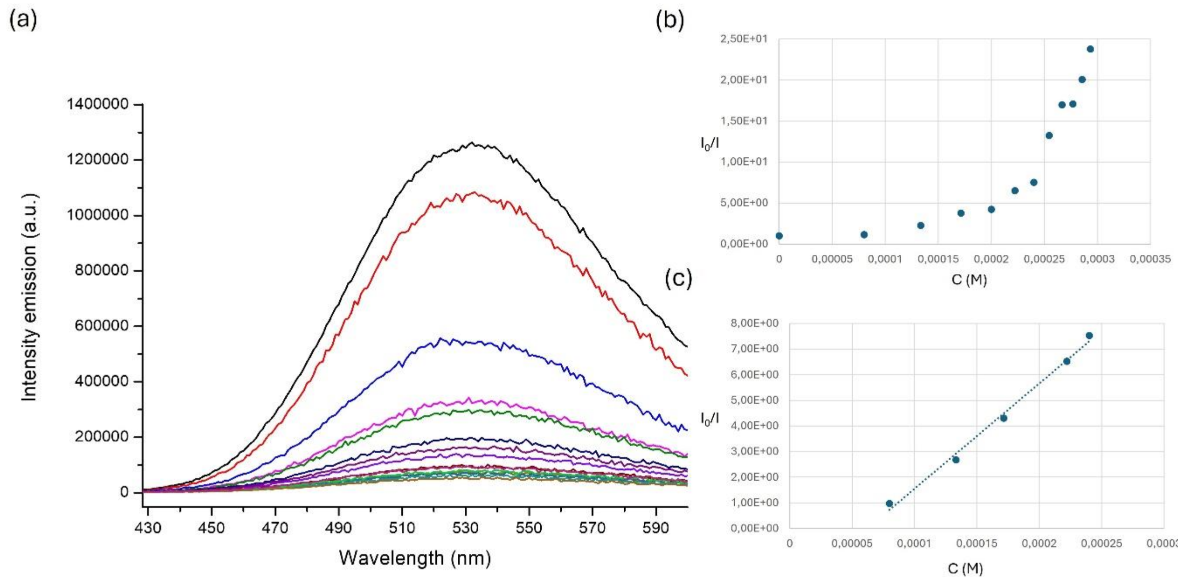

Figure S9: Emission spectra of a real river water suspension of $[Cu_4I_6(pr\text{-}ted)_2]$ submicrometric particles before and after addition TC (a). S-V plot for the quenching of the emission of the river water suspension of submicron $[Cu_4I_6(pr\text{-}ted)_2]$ particles in the presence of TC (b) and expanded Stern-Volmer plot in the linear range 0 - 2.5 µM (b).

Sensor selectivity and recyclability characterization

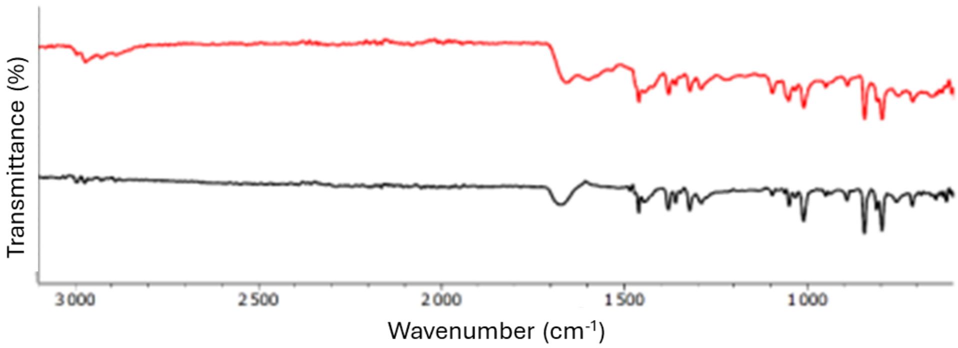

Figure S10: ATR-FTIR spectra of submicrometric $[Cu_4I_6(pr\text{-}ted)_2]$ particles (black) and after 30 cycles of immersion a TC solution (red).

DFT calculations: Fluorescence quenching mechanism to TC

Table S2. HOMO (π) and LUMO (π*) energy levels of TC.

Energy (eV)	TC
HOMO	-6.11
LUMO	-2.62
HOMO-LUMO gap	3.49

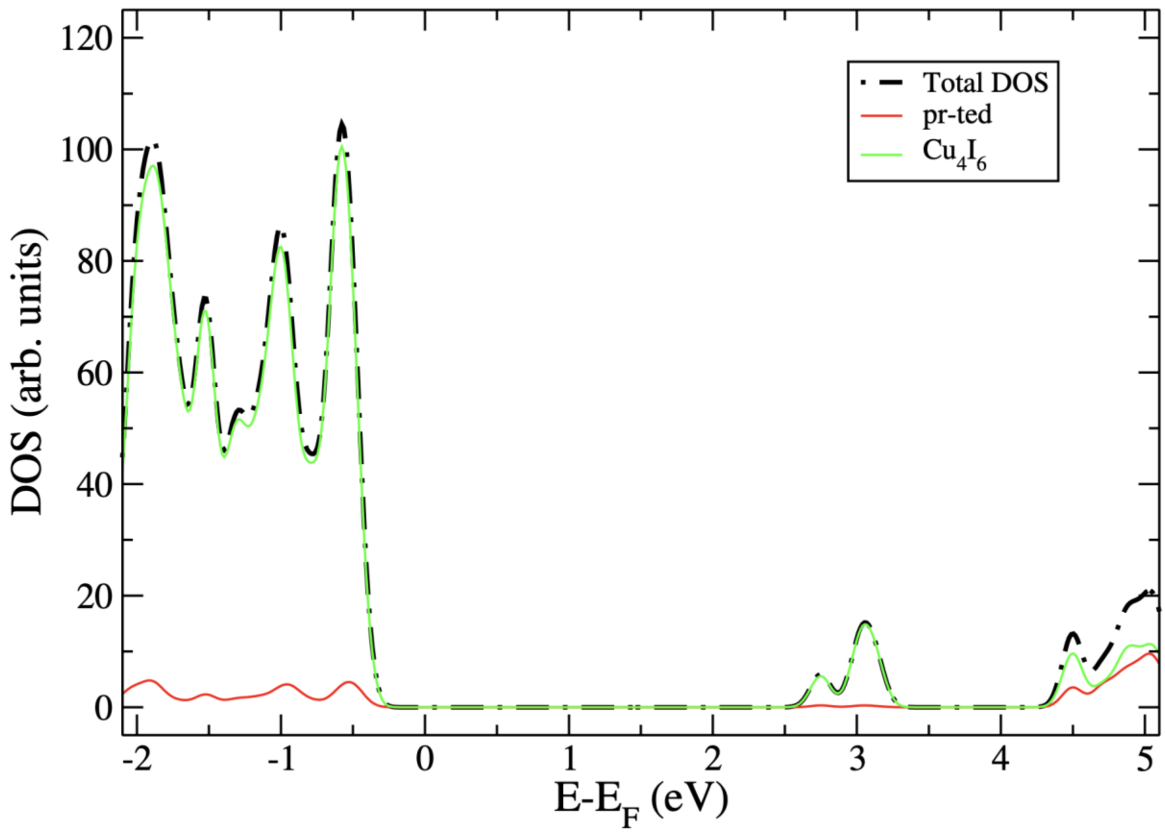

Figure S11.Total Density of States (DOS) and projections on the pr-ted and Cu_4I_6 cluster.

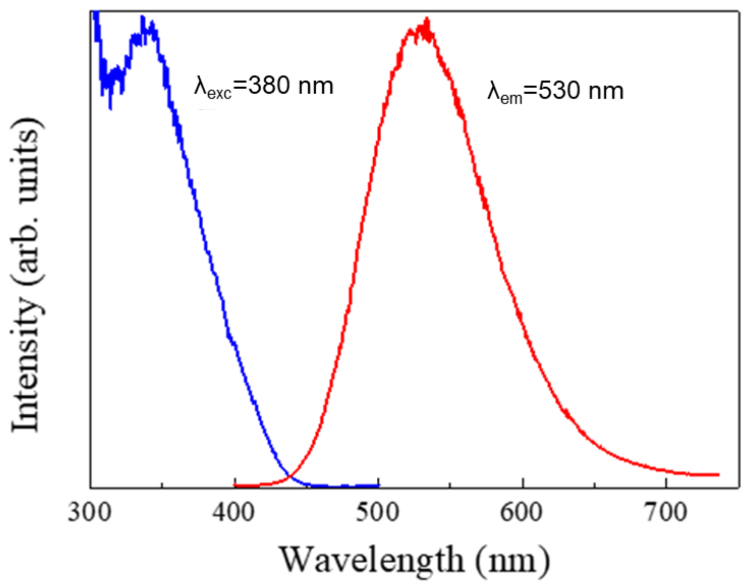

Figure S12: Emission (red), and excitation (blue) spectra of $[Cu_4I_6(pr.\text{-}ted)_2]$ particles.

Portable devices characterization.

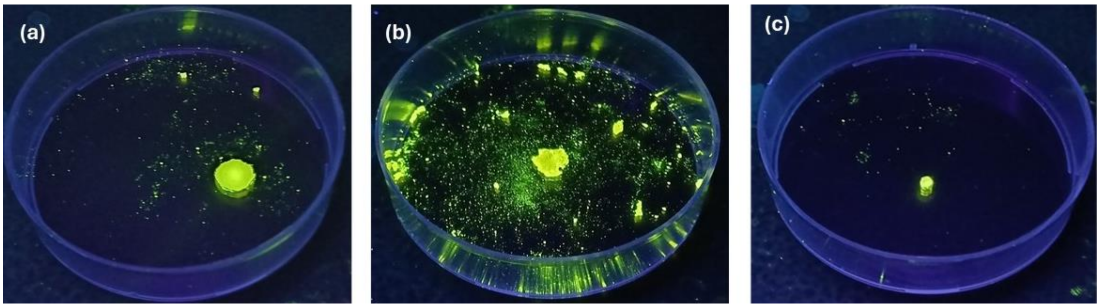

Figure S13: $[Cu_4I_6(pr\text{-}ted)_2]$ pellets formed after application of 0.4 (a), 1.4 GPa (b), and 11.1 GPa (c) of uniaxial pressure.

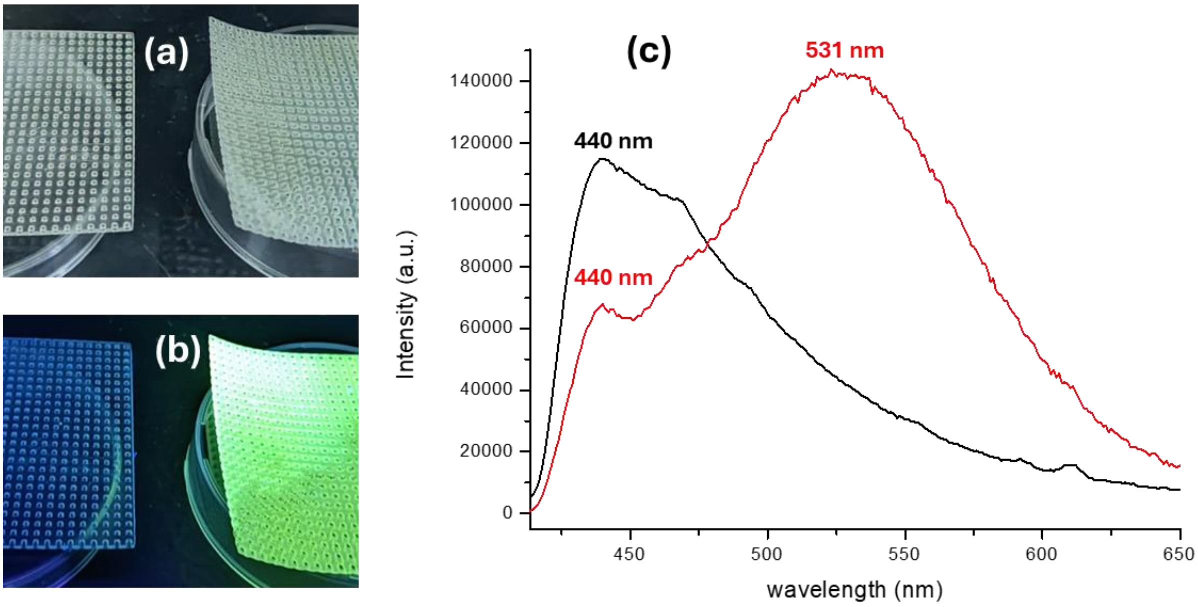

Figure S14**.** Commercial resin (left) and $[Cu_4I_6(pr\text{-}ted)_2]$@mesh0.1% (right) under visible (a) and UV (λ=365nm) light (b). Emission spectra of commercial resin (λ_{em}=440 nm, black) and $[Cu_4I_6(pr\text{-}ted)_2]$@mesh0.1% ($\lambda_{em}$=440 nm and 531 nm, red) (c).

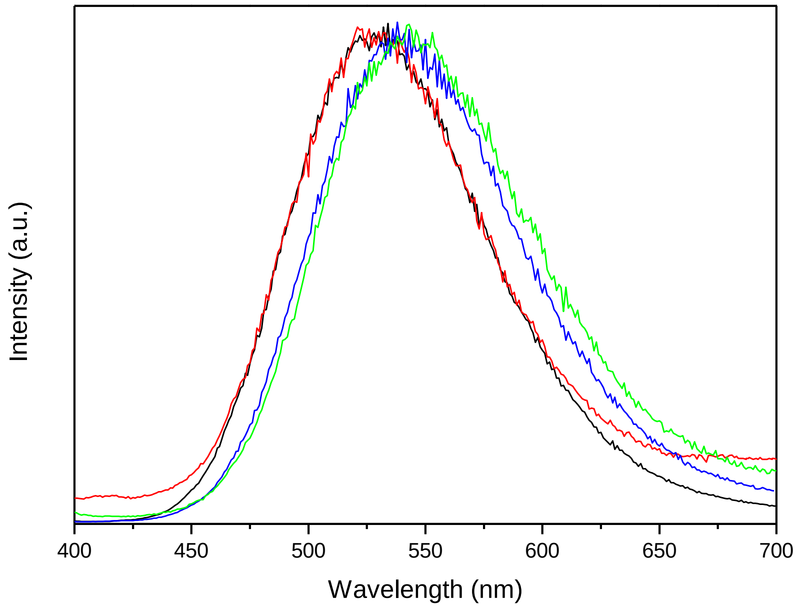

Figure S15: Emission spectra of $[Cu_4I_6(\text{pr-ted})_2]$ at ambient pressure (black) and after application of uniaxial pressure: 0.4 GPa (red), 1.4 GPa (blue) and 11.1 GPa (green).

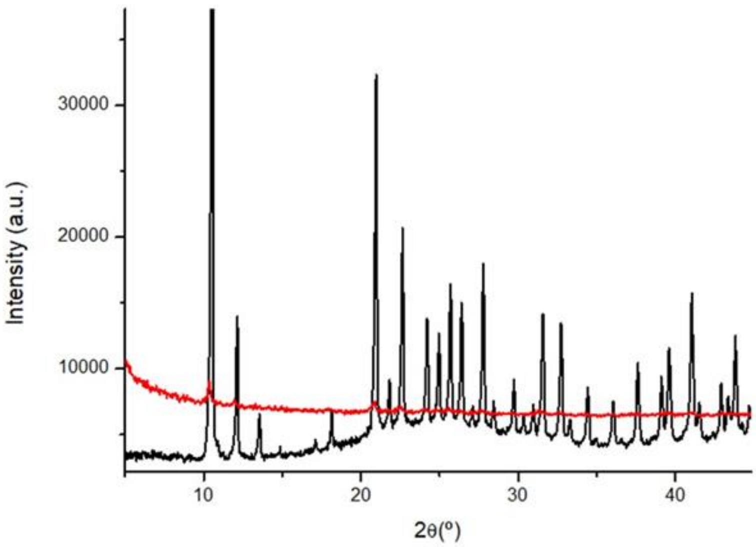

Figure S16: PXRD diffraction pattern of the submicrometric $[Cu_4I_6(\text{pr-ted})_2]$ particles (black), compared with the PXRD diffraction pattern of the submicrometric $[Cu_4I_6(\text{pr-ted})_2]$ particles pellet prepared aplying 11.1 GPa (red).

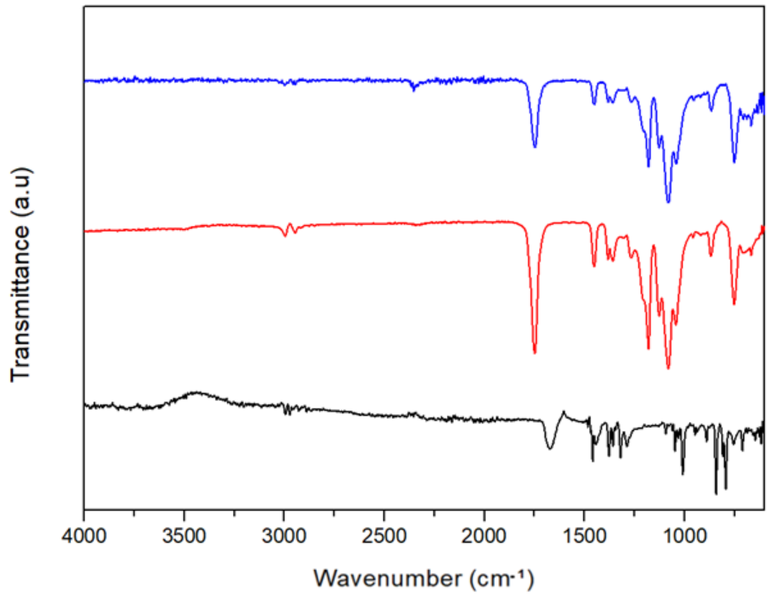

Figure S17: ATR-FTIR spectra of submicrometric [Cu_4I_6(pr-ted)$_2$] particles (black), [Cu_4I_6(pr-ted)$_2$ @PLA1%, (red) and PLA (blue).

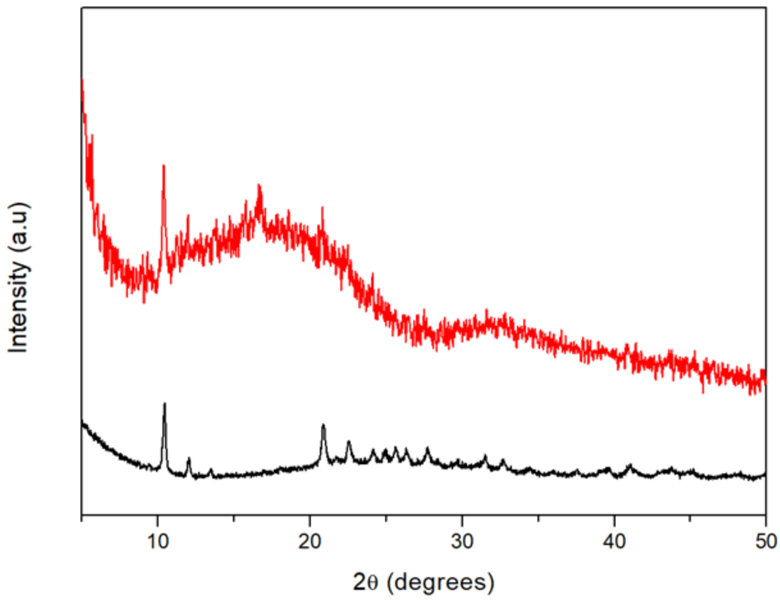

Figure S18: PXRD diffraction pattern of submicrometric [Cu_4I_6(pr-ted)$_2$] particles (black), and ([Cu_4I_6(pr-ted)$_2$ @PLA1%), (red).

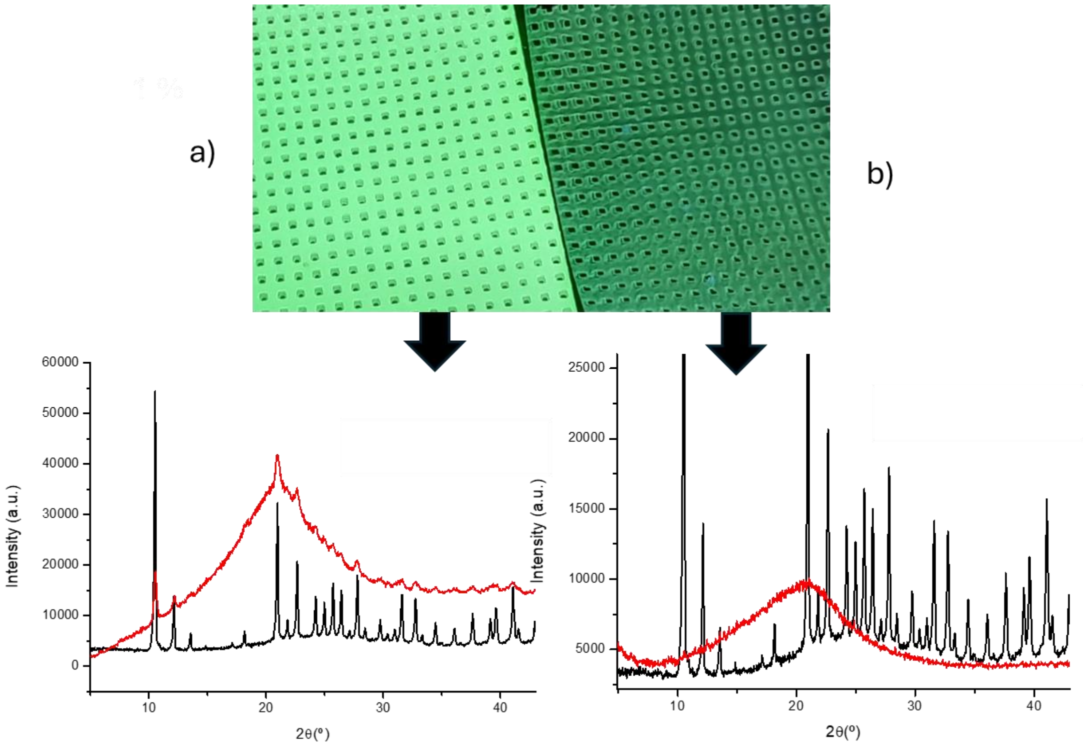

Figure S19**.** Images under UV light (λ=365nm) of $[Cu_4I_6(pr\text{-}ted)_2]$@mesh1% (top, a), and $[Cu_4I_6(pr\text{-}ted)_2]$@mesh0.1% (top, b). PXRD diffractograms of submicrometric $[Cu_4I_6(pr\text{-}ted)_2]$ particles (black), $[Cu_4I_6(pr\text{-}ted)_2]$@mesh1% (down a) and $[Cu_4I_6(pr\text{-}ted)_2]$@mesh0.1% (down b) both in red.

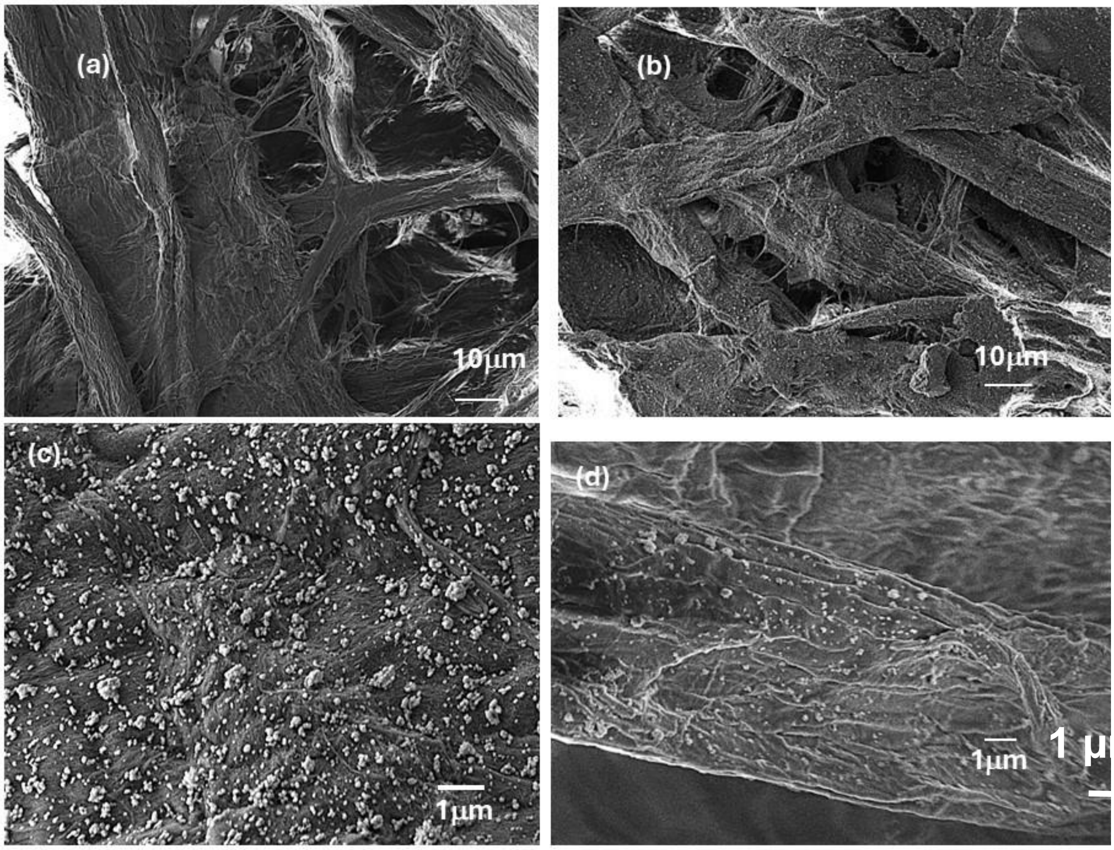

Figure S20: SEM images of the surface of uncoated paper strips (a) and of the surface (b and c) and cross section (d) of paper strips coated with $[Cu_4I_6(pr\text{-}ted)_2]$ submicrometric particles.

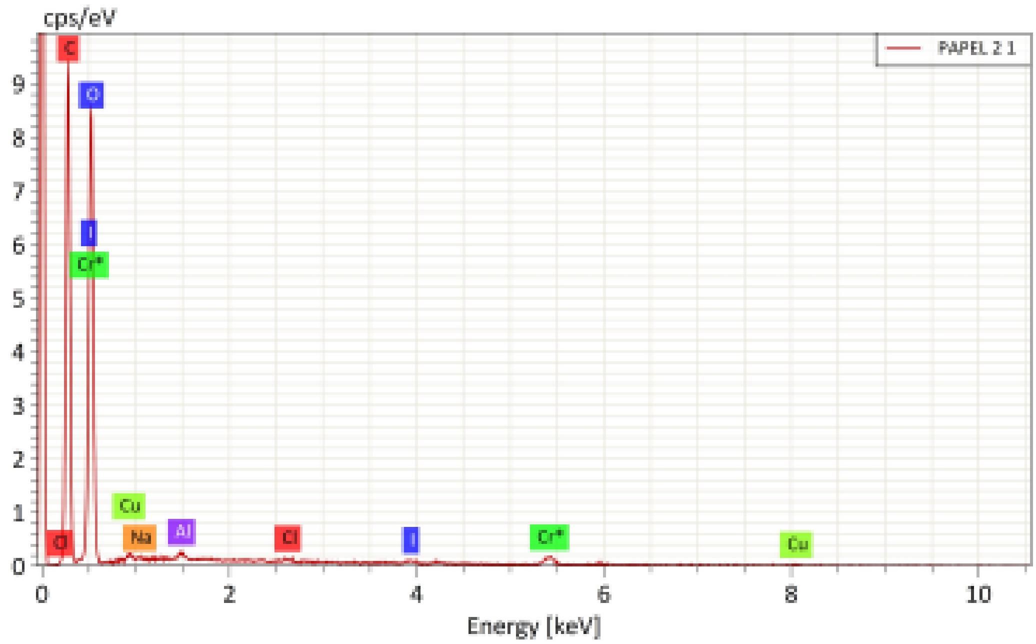

PAPEL 2 1

Element	Line series	Mass Norm. [%]	Atom [%]	abs. error [mass%] (1 σ)
C	K	45.59	53.03	2.24
O	K	53.45	46.67	2.71
Cr	K	0.00	0.00	0.00
Na	K	0.14	0.08	0.02
Al	K	0.16	0.08	0.01
Cu	K	0.23	0.05	0.03
Cl	K	0.11	0.04	0.01
I	L	0.33	0.04	0.03
		100.00	**100.00**	

Figure S21. EDX of paper strips after immersion in a submicrometric [Cu_4I_6(pr-ted)$_2$] particles suspension.

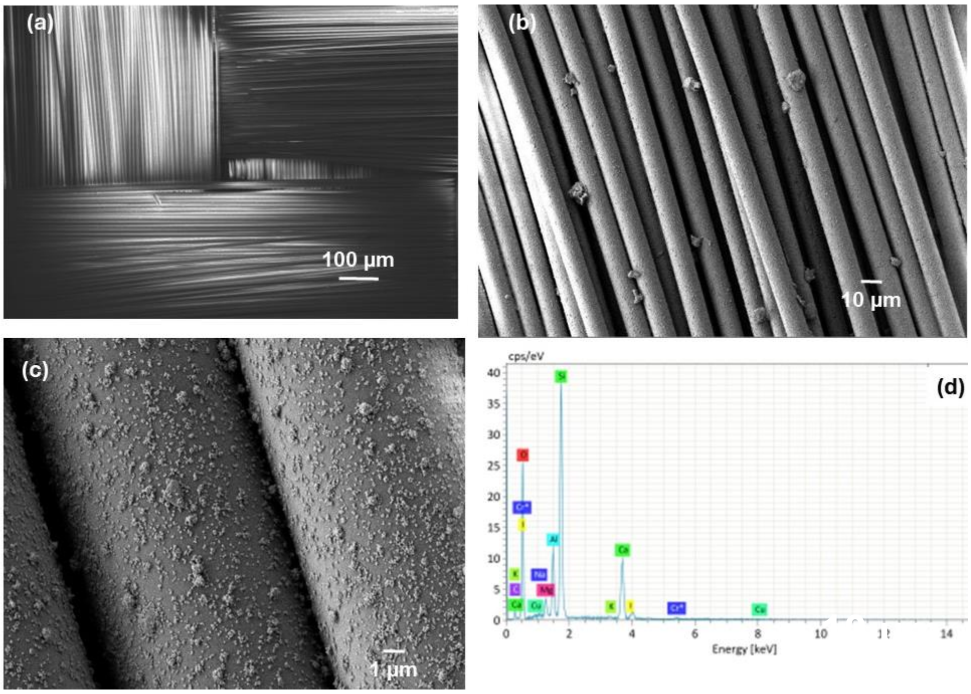

Figure S22. SEM images of glass fiber before (a) and after (b, c) immersion in a suspension of submicrometric [Cu_4I_6(pr-ted)$_2$] particles. EDX details (d).

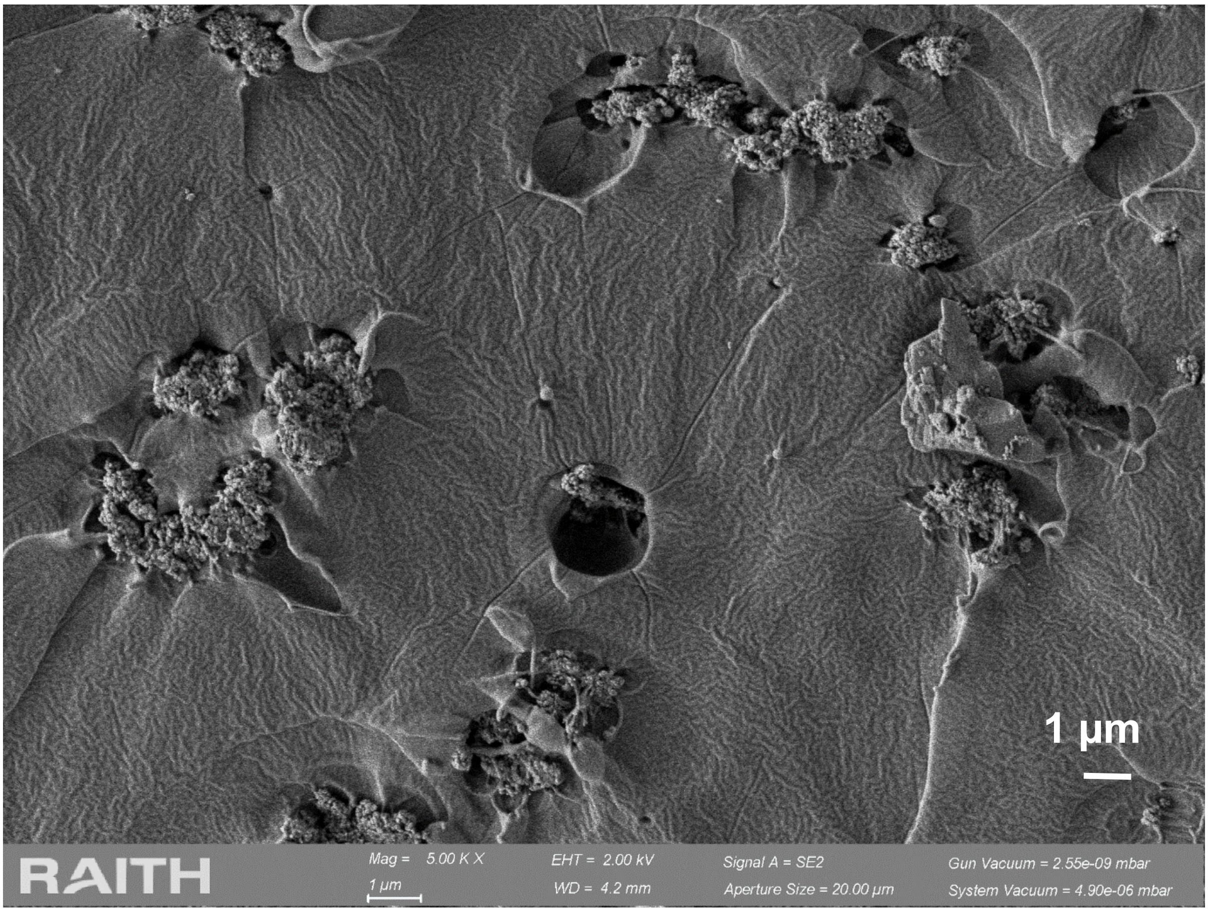
1 µm
RAITH
Mag = 5.00 K X
1 µm
EHT = 2.00 kV
WD = 4.2 mm
Signal A = SE2
Aperture Size = 20.00 µm
Gun Vacuum = 2.55e-09 mbar
System Vacuum = 4.90e-06 mbar

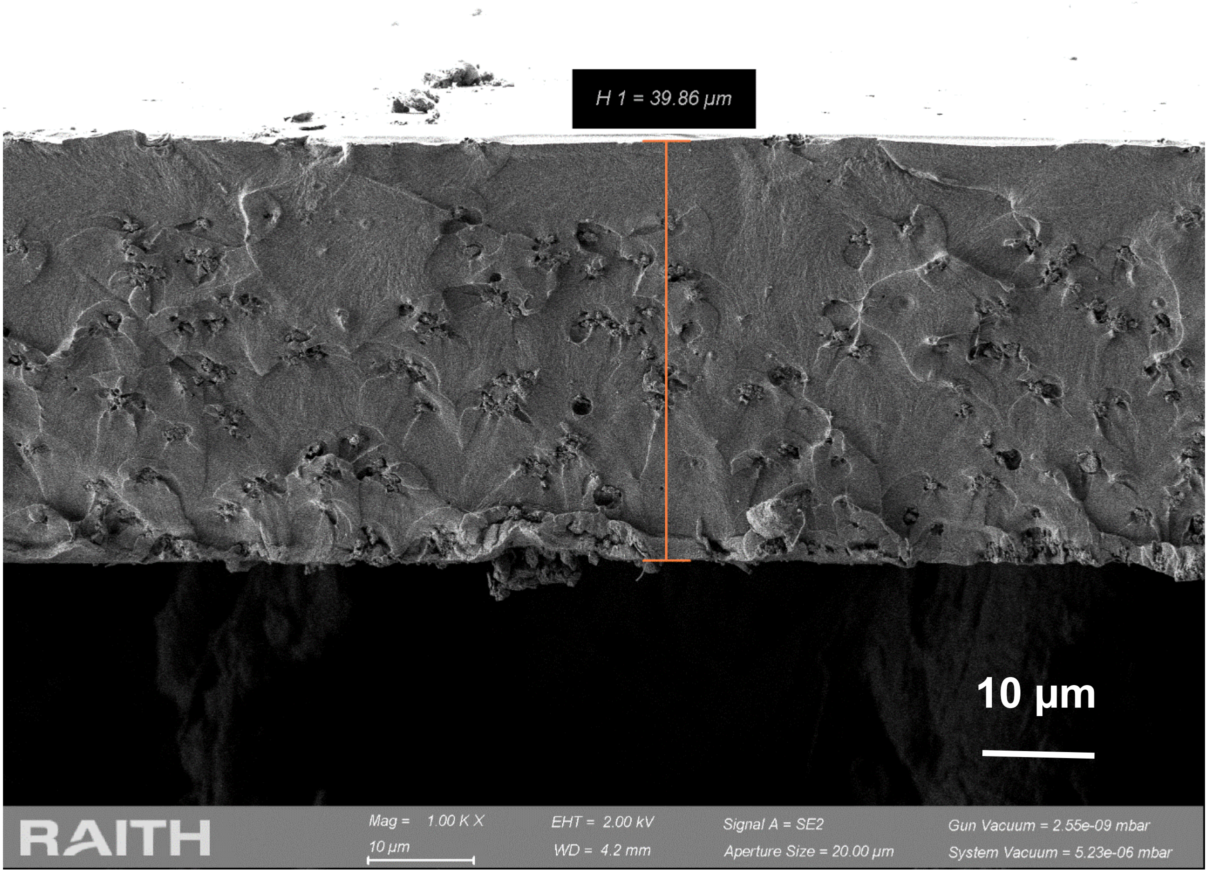
H 1 = 39.86 µm
10 µm
RAITH
Mag = 1.00 K X
10 µm
EHT = 2.00 kV
WD = 4.2 mm
Signal A = SE2
Aperture Size = 20.00 µm
Gun Vacuum = 2.55e-09 mbar
System Vacuum = 5.23e-06 mbar

Figure S23: SEM images of [Cu_4I_6(pr-ted)$_2$]@PLA1%, (top) and cross section (bottom).

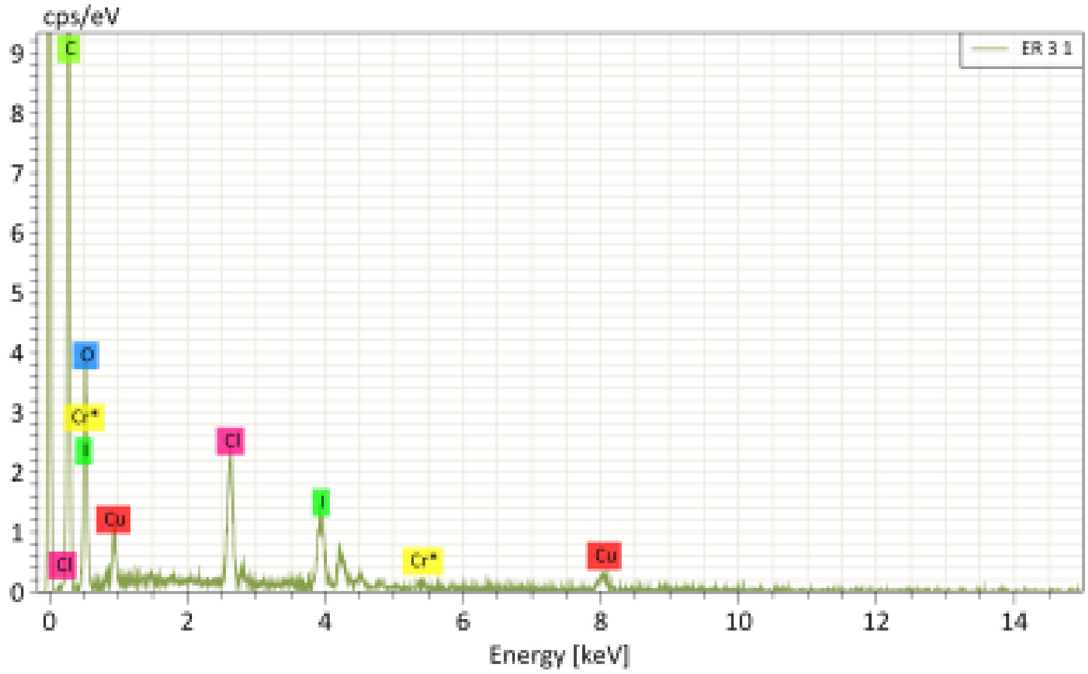

ER 3 1

Element	Line series	Mass Norm. [%]	Atom [%]	abs. error [mass%] (1 σ)
C	K	57.28	72.41	3.43
O	K	25.13	23.86	1.64
Cl	K	3.95	1.69	0.31
I	L	10.21	1.22	0.83
Cu	K	3.44	0.82	0.41
Cr	K	0.00	0.00	0.00
		100.00	**100.00**	

Figure S24: EDX of [Cu_4I_6(pr-ted)$_2$]@PLA1%.

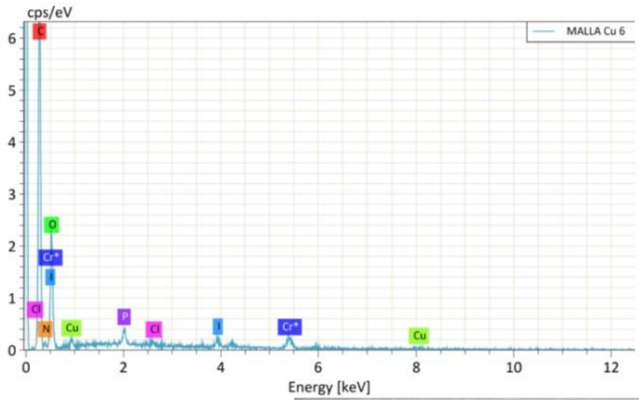

MALLA Cu 6

Element	Line series	Mass Norm. [%]	Atom [%]	abs. error [mass%] (1 σ)
C	K	56.61	64.57	2.79
O	K	33.16	28.39	1.83
N	K	6.42	6.28	0.57
P	K	0.70	0.31	0.06
I	L	2.25	0.24	0.17
Cu	K	0.73	0.16	0.11
Cl	K	0.12	0.05	0.02
Cr	K	0.00	0.00	0.00
		100.00	100.00	

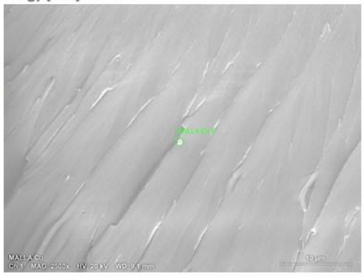

Figure S25: SEM-EDX of $[Cu_4I_6(\text{pr-ted})_2]$@mesh0.1%.

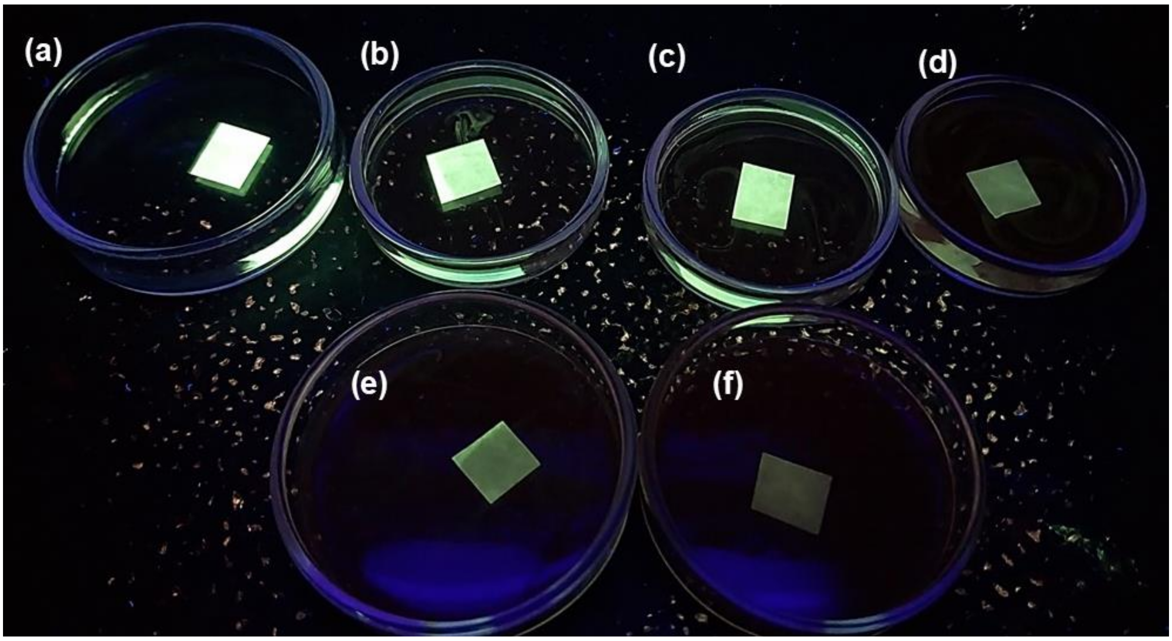

Figure S26: Image of paper strips coated with submicrometric particles submerged in different concentrations of TC under UV light (λ = 365 nm). 0 μM (a), 50 μM (b), 100 μM,(c), 200 μM,(d), 300 μM (e), and 400 μM (f).